Molecular Therapy
Methods & Clinical Development
Original Article

Novel *GAA* Variants and Mosaicism in Pompe Disease Identified by Extended Analyses of Patients with an Incomplete DNA Diagnosis

Stijn L.M. in 't Groen,[1,2,3] Douglas O.S. de Faria,[1,2,3] Alessandro Iuliano,[1,2,3] Johanna M.P. van den Hout,[1,3] Hannie Douben,[2] Trijnie Dijkhuizen,[4] David Cassiman,[5] Peter Witters,[5] Miguel-Ángel Barba Romero,[6] Annelies de Klein,[2] Galhana M. Somers-Bolman,[2] Jasper J. Saris,[2] Lies H. Hoefsloot,[2] Ans T. van der Ploeg,[1,3] Atze J. Bergsma,[1,2,3] and W.W.M. Pim Pijnappel[1,2,3]

[1]Department of Pediatrics, Erasmus University Medical Center, 3015 GE Rotterdam, the Netherlands; [2]Department of Clinical Genetics, Erasmus University Medical Center, 3015 GE Rotterdam, the Netherlands; [3]Center for Lysosomal and Metabolic Diseases, Erasmus University Medical Center, 3015 GE Rotterdam, the Netherlands; [4]Department of Genetics, University of Groningen, University Medical Center Groningen, 9713 GZ Groningen, the Netherlands; [5]Center for Metabolic Diseases, UZ and KU Leuven, 3000 Leuven, Belgium; [6]Internal Medicine Department, Albacete University Hospital, 02006 Albacete, Spain

Pompe disease is a metabolic disorder caused by a deficiency of the glycogen-hydrolyzing lysosomal enzyme acid α-glucosidase (GAA), which leads to progressive muscle wasting. This autosomal-recessive disorder is the result of disease-associated variants located in the *GAA* gene. In the present study, we performed extended molecular diagnostic analysis to identify novel disease-associated variants in six suspected Pompe patients from four different families for which conventional diagnostic assays were insufficient. Additional assays, such as a generic-splicing assay, minigene analysis, SNP array analysis, and targeted Sanger sequencing, allowed the identification of an exonic deletion, a promoter deletion, and a novel splicing variant located in the 5′ UTR. Furthermore, we describe the diagnostic process for an infantile patient with an atypical phenotype, consisting of left ventricular hypertrophy but no signs of muscle weakness or motor problems. This led to the identification of a genetic mosaicism for a very severe GAA variant caused by a segmental uniparental isodisomy (UPD). With this study, we aim to emphasize the need for additional analyses to detect new disease-associated *GAA* variants and non-Mendelian genotypes in Pompe disease where conventional DNA diagnostic assays are insufficient.

INTRODUCTION

Pompe disease (glycogen storage disease type II, OMIM 232300) is a rare metabolic disorder that leads to progressive muscle wasting caused by acid α-glucosidase (GAA) enzyme deficiency. This autosomal-recessive disorder is caused by disease-associated variants located in the *GAA* gene.[1] Classic infantile Pompe patients have a complete deficiency of GAA enzymatic activity and present hypertrophic cardiomyopathy and severe muscle weakness shortly after birth. Patients with residual GAA activity can be classified as childhood- or adult-onset Pompe patients, based on the age at symptom onset, and generally do not show cardiac involvement.

Enzyme replacement therapy (ERT) is currently the only available treatment. Without treatment, classic infantile Pompe patients do not survive the first year of life due to cardiorespiratory failure.[2,3] In order to become eligible for ERT, a patient needs to present a clinical phenotype related to Pompe disease and have a GAA deficiency, and certain countries require the identification of two disease-associated variants in the *GAA* gene.[4] GAA activity measurements are performed using dried blood with spot sampling or with primary fibroblasts or leukocytes using either glycogen or 4-methylumbelliferone-α-d-glucopyranoside (4MU) as a substrate.[5] False-positive results are known to occur using blood-based assays, for example, those caused by known pseudodeficiency alleles; therefore, DNA analysis is recommended in order to identify disease-associated variants.[5–7] Routine diagnostic DNA analysis usually focuses only on the coding regions of *GAA* using PCR reactions and subsequent Sanger sequencing.[6,8] This method detects variants in the coding regions and in close proximity to splice sites but not in the promoter, UTRs, and most of the intronic regions.[4,9] Reported variants are listed in the "Pompe disease *GAA* variant database" (http://www.pompevariantdatabase.nl), which contains over 400 disease-associated variants in *GAA* and has4 recently been extended to include clinical phenotypes.[10] When the disease-associated variants of both alleles are identified using DNA sequencing, a general prediction of the patient phenotype is possible using the information in this database. Recent findings indicate that analysis of the modifier c.510C> T variant, which is silent but modulates splicing in patients carrying the common c.-32-13T>G (IVS1) variants, is also important.[11]

Received 9 November 2019; accepted 31 December 2019;
https://doi.org/10.1016/j.omtm.2019.12.016.

Correspondence: W.W.M. Pim Pijnappel, Department of Clinical Genetics, Erasmus University Medical Center, Wytemaweg 80, Rotterdam 3015 CN, the Netherlands.
E-mail: w.pijnappel@erasmusmc.nl

Table 1. Basic Information for All Patients at Start of Analysis

	Age at Symptom Onset	GAA Activity in Fibroblasts (Patient Range: 0–20 nmol/h/mg)	Disease-Associated Variant 1	Disease-Associated Variant 2	Initial Symptoms
Patient 1	<1 month	0 nmol/h/mg	c.2331+2T>A p.0?	?	muscle weakness and cardiomyopathy
Patient 2	15 years	13.7 nmol/h/mg	c.-32-13T>G p.=, p.0?	?	muscle weakness
Patient 3 (sibling 1)	24 years	7.5 nmol/h/mg	? + c.2065G>A ? + p.(Glu689Lys)	? + c.2065G>A ? + p.(Glu689Lys)	general fatigue
Patient 4 (sibling 2)	41 years	deficient in lymphocytes	? + c.2065G>A ? + p.(Glu689Lys)	? + c.2065G>A ? + p.(Glu689Lys)	muscle weakness and general fatigue
Patient 5 (sibling 3)	21 years	deficient in lymphocytes	? + c.2065G>A ? + p.(Glu689Lys)	? + c.2065G>A ? + p.(Glu689Lys)	muscle weakness and general fatigue
Patient 6	<1 month	8.1 nmol/h/mg	c.925G>A p.(Gly309Arg)	?	left ventricular hypertrophy

Previously, we described an exon-flanking RT-PCR that can be used to detect novel disease-associated variants that affect pre-mRNA splicing, irrespective of their location.[9,12] This assay is important for diagnosis but also to allow the design of antisense oligonucleotides that can restore splicing.[12–15] Other work has shown single-nucleotide polymorphism (SNP) array analysis to be capable of explaining phenotypes by detecting large deletions or genomic copy number variations (CNVs).[16–18] In addition, SNP array analysis can be used to elucidate homozygote variants incompatible with Mendelian inheritance by detecting uniparental isodisomies (UPDs) and regions of homozygosity (RoHs).[16,17]

Here, we utilized the additional diagnostic assays described above to identify the genetic cause of Pompe disease in six patients from four families with incomplete DNA sequencing results. This resulted in the identification of three novel disease-associated variants located in non-coding regions of *GAA*. Additionally, we describe the genetic analysis performed for a patient with an atypical Pompe phenotype, first described in Labrijn-Marks et al.[17] We provide the clinical symptoms and the series of experiments that were performed in order to make this diagnosis and to strengthen the conclusion that this is a mosaic patient.

RESULTS

The six patients (including three siblings) described here had symptoms that could be attributed to a GAA deficiency. Enzymatic activity of GAA was found deficient in primary fibroblasts and indicated that Pompe disease is a probable cause of symptoms. Genetic screenings of the coding regions of GAA were insufficient to provide a genotype that corresponds with the observed phenotype (Table 1).

Patient 1

The first indication of Pompe disease was observed during prenatal ultrasound, which found evidence of cardiac hypertrophy. Muscle weakness presented shortly after birth, and cultured primary fibroblasts showed no GAA enzyme activity (Table 1). Sanger sequencing of the coding regions identified the heterozygous c.2331+2T>A variant (Table 1; Figure 1A). The intronic c.2331+2T>A variant has been classified as "very severe" and is associated with the classic infantile phenotype when combined with a null allele.[10,19] This variant is located close to the exon 16 splice donor site and affects splicing of intron 16, ultimately resulting in a frameshift, the generation of an early stop codon, and mRNA degradation. The second disease-associated variant was not identified by standard DNA sequencing.

Exon-flanking RT-PCR for all *GAA* exons was performed as previously described[9] to test for the presence of a non-coding intronic variant and revealed an aberrant product of exons 8, 9, and 10 (Figure 1B; product 2). Sanger sequence analysis of this product showed the exclusion of exon 9 from the transcripts, but it failed to identify a candidate splicing variant around the splice junctions (Figure 1C). To test the possibility of a deletion that could have been obscured by the presence of the other allele, we performed flanking exon PCR analysis of exon 9 (ranging from exon 8 to exon 10) using genomic DNA as a template (Figure 1D). This showed the presence of an additional band in the patient DNA that was not found in the healthy control, one that corresponded with the expected product ranging from exon 8 to 10 and one that contained a 343-bp deletion that spanned exon 9 and parts of the neighboring introns (band A in Figure 1E).

The resulting c.1327-61_1437+171del variant explains the exclusion of exon 9 at the RNA level and why the initial DNA sequencing analysis was unable to detect this variant, as the annealing sites for PCR amplification were included in the deleted region. The deletion of exon 9 has been shown to result in a total disruption of GAA enzyme activity in previous work.[9] The combination of c.1327-61_1437+171del and c.2331+2T>A explains the lack of enzyme activity and the classic infantile phenotype of the patient (Figure 1F).

Patient 2

The second patient presented mild muscle weakness at 15 years of age. GAA activity in fibroblasts was found to be reduced to 13.7 nmol/h/mg (patient range: 0–20 nmol/h/mg). Sanger sequencing analysis performed on the patient's DNA identified the c.-32-13T>G

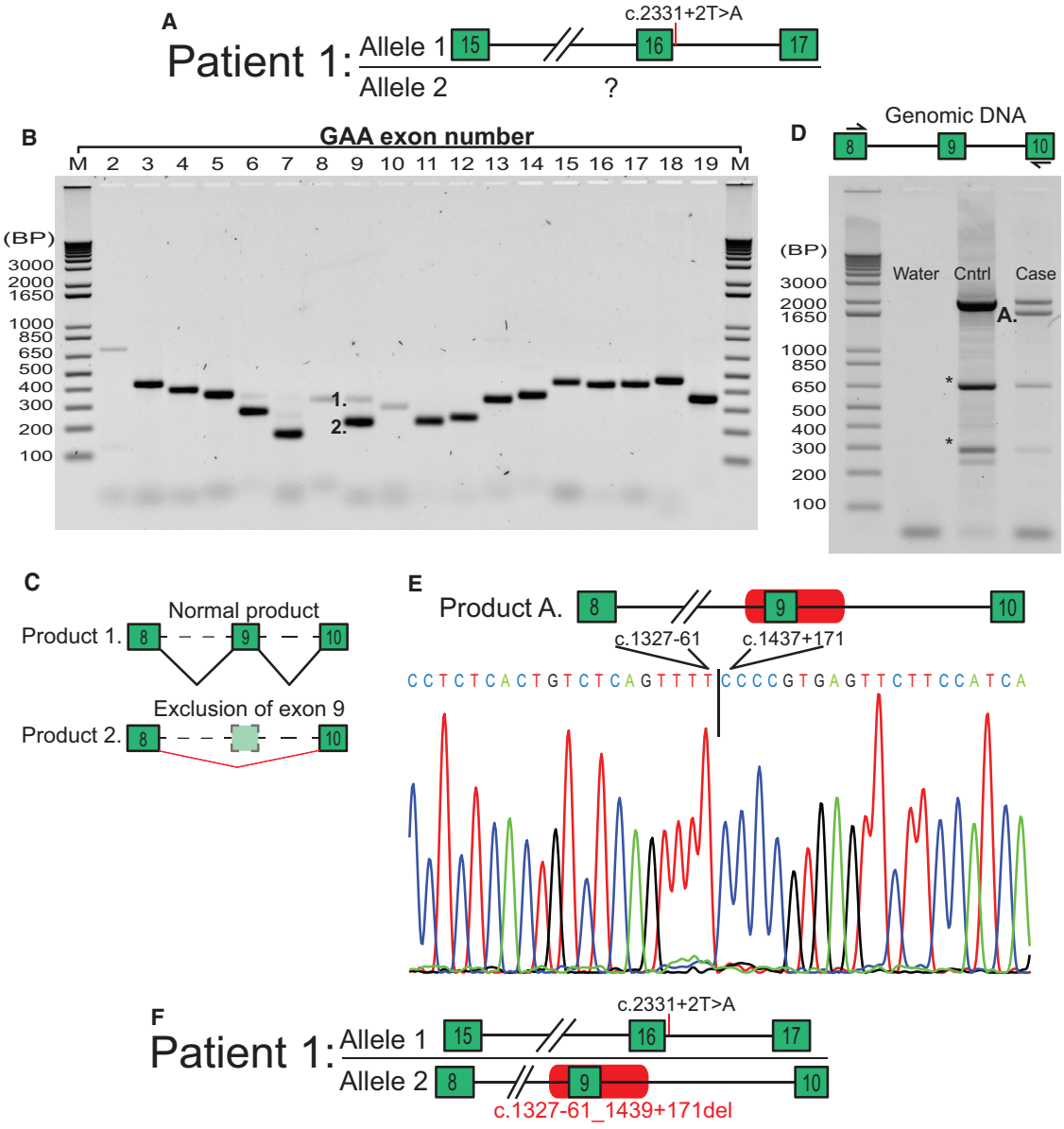

Figure 1. Identification of a Disease-Associated Deletion in Patient 1 Using the Splicing Assay

(A) Genotype of patient 1 at the start of analysis. (B) Splicing assay for *GAA* exons 2–19 performed on cDNA obtained from fibroblasts. Bands marked 1. and 2. indicate two different products detected around exon 9. (C) Cartoons of products 1 and 2 identified using Sanger sequencing of the PCR product. (D) PCR product from *GAA* exon 8 to exon 10, performed on DNA. A., An additional band from patient 1 that was 343 bp smaller compared to the normal product; *, non-specific bands as a result of the PCR. (E) Sanger sequencing of product A. The new junction resulting from the deletion is indicated. (F) Cartoon of both disease-associated variants identified in patient 1.

(IVS1) variant in a heterozygous state but failed to identify a second disease-associated variant (Table 1; Figure 2A)

Exon-flanking RT-PCR of cDNA, derived from the patient's fibroblasts, showed no aberrant splicing products, except for those caused by the IVS1 variant around exon 2 (Figure 2B).[13,20,21] Next, we performed SNP array analysis to test for the presence of large genomic aberrations. This analysis revealed a deletion on chromosome 17 (GRCh37/hg19 [Chr17:78.059.821–78.076.592]) (Figure 2C). Further evaluation of this 17kb deletion indicated that it starts upstream of *GAA* in the *CCDC40* gene and included the promoter, transcription start site (TSS), and non-coding exons 1A and 1B of *GAA*.

Formally proving the pathogenicity of this deletion was complicated, due to the residual GAA expression and activity originating

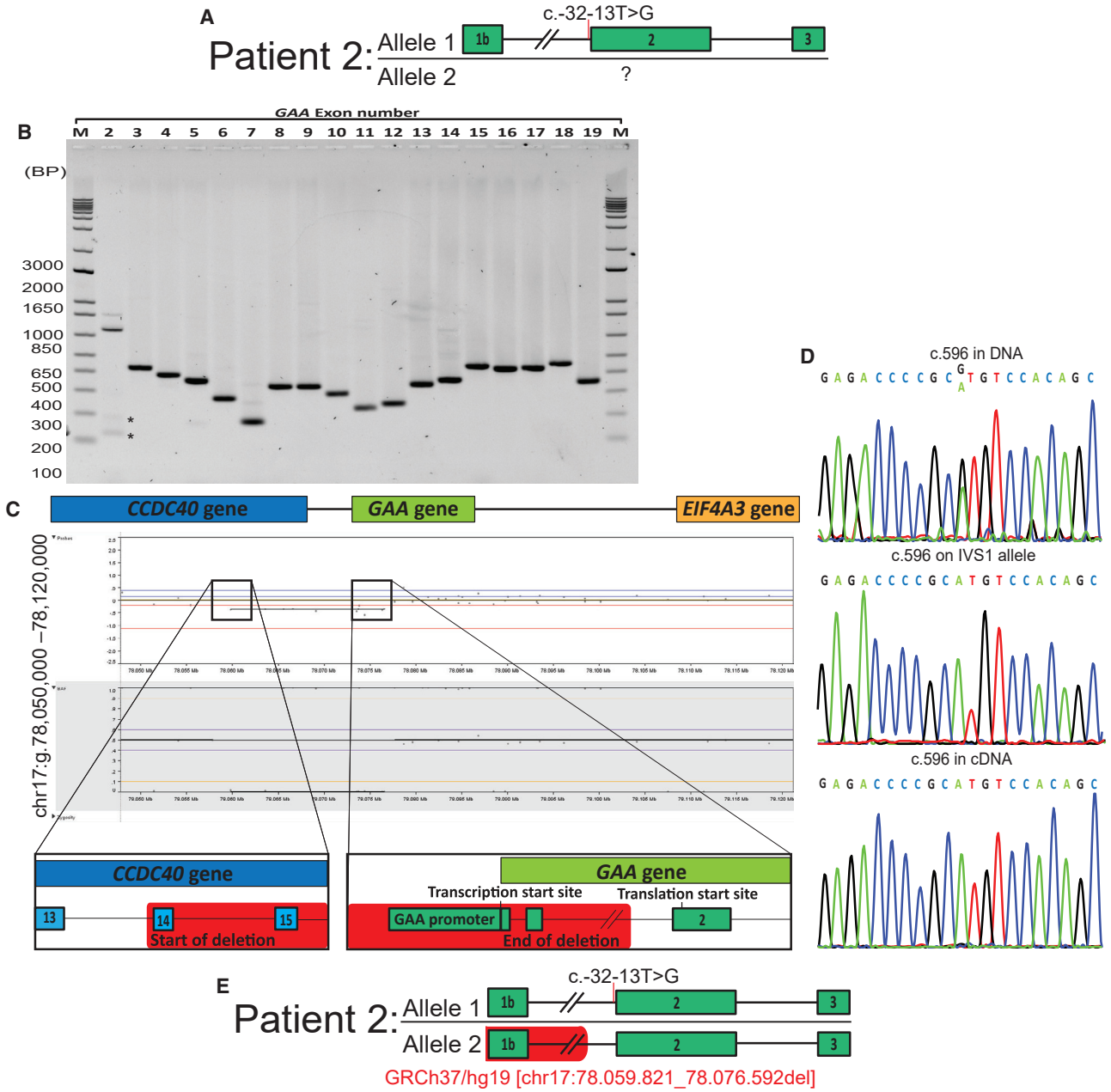

Figure 2. Identification of a *GAA* Promoter Deletion in Patient 2 Using a SNP Array

(A) Genotype of patient 2 at the start of analysis. (B) Splicing assay for *GAA* exons 2–19 performed on cDNA obtained from fibroblasts. *Known mis-spliced transcripts caused by the IVS1 variant. (C) Cartoon of the genomic region spanning the *CCDC40*, *GAA*, and *EIF4A3* genes in the chromosome (top) and the SNP array analysis (bottom) visualized for Chr17:78,050,000–78,120,000. Zooms are also shown on the 5′ and 3′ ends of the 17-kb deletion. (D) Sanger sequencing results around the c.596A>G SNP using a non allele-specific PCR of DNA (top), an IVS1 allele-specific PCR of DNA (middle), and a non allele-specific PCR of cDNA obtained from fibroblasts (bottom). (E) Cartoon of both disease-associated variants identified in patient 2.

from the IVS1 allele. To address this, the sequence of exon 3 in the patient's DNA and mRNA was analyzed for allele-specific SNPs (Figure 2D). We identified the c.596A>G SNP (rs1042393, minor allele frequency [MAF] in Dutch population: 75%) in a heterozygous state in the patient's DNA.[22] With the use of an IVS1-specific PCR (Figure S1), we found the c.596A>G SNP not to be present on the allele containing the IVS1 variant. Sequence analysis of the cDNA failed to detect transcripts that contained the c.596A>G SNP, indicating that the allele containing the deletion is not expressed.

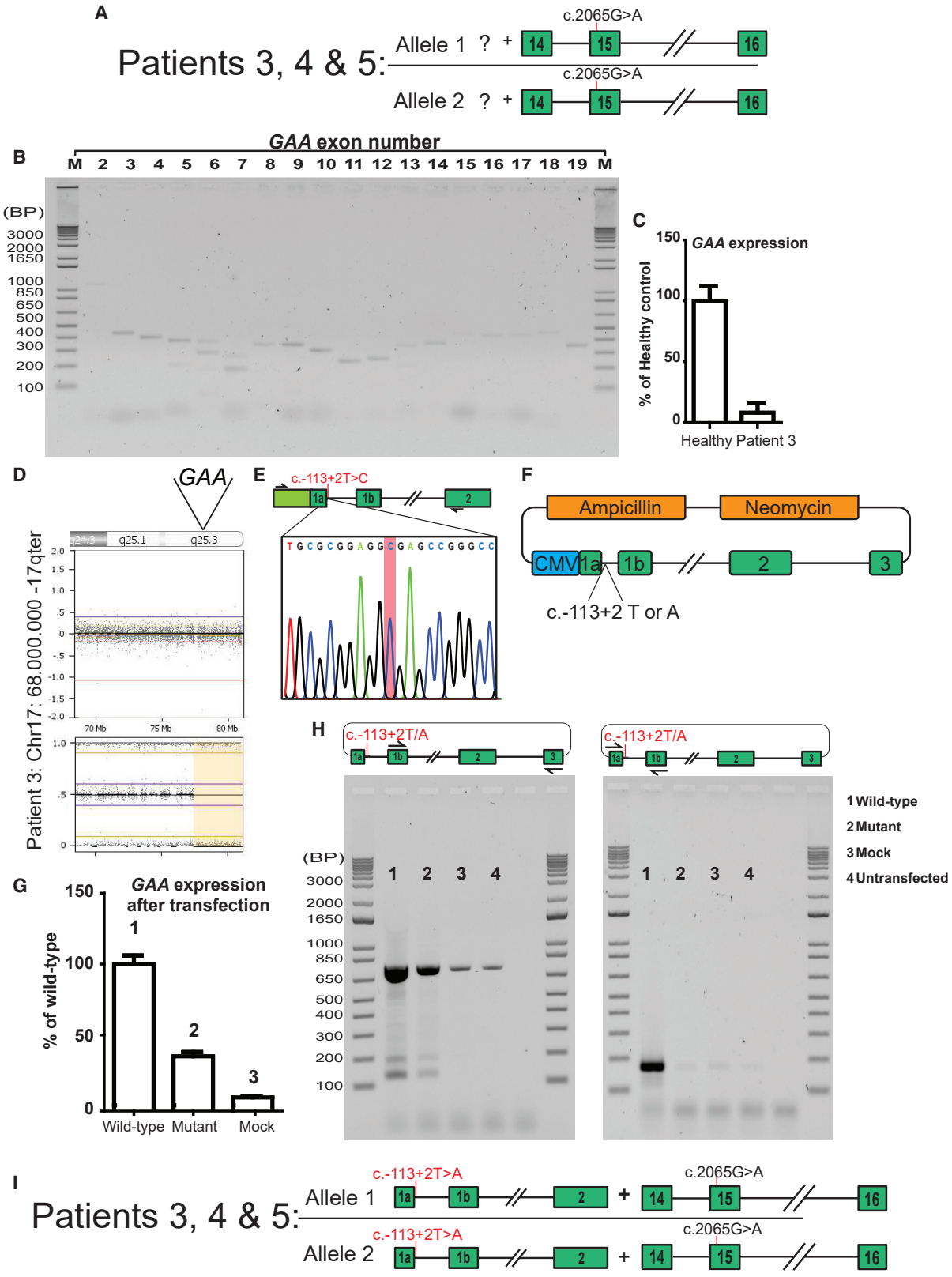

(legend on next page)

In conclusion, the 17kb deletion, including the promoter and TSS, completely abrogates *GAA* expression, and the combination with the late-onset IVS1 variant on the other allele (Figure 2E) explains the late-onset phenotype presented by the patient.

Patients 3, 4, and 5

Patients 3, 4, and 5 are siblings, all of whom showed progressive muscle weakness later in life. Primary fibroblasts were only available for patient 3. GAA activity in lymphocytes was deficient in all three siblings; this was confirmed in the primary fibroblasts of patient 3 (Table 1). Sanger sequence analysis revealed the 2065G>A variant in a homozygous state for all three siblings but was unable to identify any disease-associated variants (Figure 3A). Previous work has shown that the c.2065G>A variant reduces GAA activity to 54% in a *GAA* cDNA expression construct.[23] This reduction is not sufficient for a patient to present symptoms associated with Pompe disease but is known to lead to a pseudodeficiency of GAA.[23]

Exon-flanking RT-PCR of cDNA derived from fibroblasts of patient 3 did not detect any aberrant splicing events but showed an overall low expression of *GAA* (Figure 3B). Quantitative real-time PCR (qRT-PCR) analysis confirmed this, showing a reduction of *GAA* expression to 8% of healthy control values (Figure 3C). SNP array analysis showed several large RoHs in all siblings that were likely derived from regions that were homologous in both parents, suggesting consanguinity between the parents. Interestingly, all three siblings were found to have a RoH ranging from 17q25.3 to the 17qter (including *GAA*) but this was not present in the paternal DNA (Figure 3D; Figure S2). The consanguinity of the parents explains the presence of the multiple RoHs in the three siblings via a combination of several identical blocks. However, this finding does not explain the decreased expression of *GAA* mRNA, and we hypothesized the presence of a variant in the 5′ UTR or the promoter. To this end, Sanger sequencing was performed for the non-coding first exons and the *GAA* promoter (Figure 3E). Sanger sequence analysis of this region revealed the presence of the homozygous variant c.-113+2T>A in patient 3. This variant is located close to the splice acceptor of exon 1A, which is, according to recent annotations, the 5′ part of exon 1. Our unpublished RNA sequencing (RNA-seq) data indicate that in agreement with the recent annotations, exon 1 consists of two small exons (exon 1A and exon 1B) that are spliced in cells from healthy individuals, as well as patients with Pompe disease. The c.-113+2T>A variant was also found in a homozygous state in the two siblings (patients 4 and 5) and in a heterozygous state in paternal DNA. This variant has not been described previously. DNA from the mother was unavailable.

To investigate the pathogenic nature of c.-113+2T>A, a previously published minigene model was modified to include the genomic region of exon 1A.[12] Two new constructs were generated, one wild-type and one carrying the c.-113+2T>A variant (Figure 3F). qRT-PCR of cDNA obtained from transfected HEK293T cells using primers located in exon 2 showed that c.-113+2T>A reduced *GAA* expression to 35% of the wild-type minigene (Figure 3G). Exon-flanking PCR for exons 1 to 3 showed that c.-113+2T>A lowered expression of mRNA containing exon 1B-exon 3 (Figure 3H, left panel). An additional exon-flanking RT-PCR was performed to detect aberrant splicing events between exons 1A and 1B (Figure 3H). The wild-type construct spliced both exons correctly, whereas the mutant completely abolished expression of the mRNA transcript containing the exon 1A-exon 1B splice junction (Figure 3H). We note that we were unable to test these splicing events in patient fibroblasts due to the low expression of GAA mentioned previously.

In summary, the c.-113+2T>A variant decreases expression of *GAA*. We note that the reduction in the minigene was less strong (65%) compared to the reduction in fibroblasts (92%). This difference might be due to promoter-dependent effects of the c.-113+2T>A variant, as in the patient's fibroblasts, mRNA expression is regulated by the endogenous *GAA* promoter, whereas expression from the minigene model is regulated by the cytomegalovirus (CMV) promoter. Additionally, all three patients carry both the c.-113+2T>A and c.2065G>A variants at a homozygous state (Figure 3I). The c.2065G>A missense variant is known to decrease activity to ~50%.[23] The combined action of both variants likely reduces endogenous GAA activity to pathogenic levels.

Patient 6

Indications for a superior vena cava syndrome were found during a routine prenatal ultrasound. Further cardiac screening was performed at the age of 2.5 months and revealed a left ventricular hypertrophy (LVH) with cardiac ultrasound, whereas electrocardiography showed a shortened PQ interval time without signs of pre-excitation (Table 2). At this time, the patient was normotonic with good psychomotor development and showed no signs of muscle weakness. Exome screening of cardiac genes was negative, and a metabolic examination of plasma and urine showed mildly elevated creatine kinase (CK) and transaminase levels. GAA activity was found to be only slightly

Figure 3. Identification of a RoH and a Novel Splicing Variant in Exon 1A in Patients 3–5

(A) Genotype of patient 3 at the start of analysis. (B) Splicing assay for *GAA* exons 2–19 performed on cDNA obtained from fibroblasts from patient 3. (C) qRT-PCR results for *GAA* performed on cDNA obtained from fibroblasts, normalized for *GAPDH*. Significance comparing healthy control and patient 3: $p < 0.001$. (D) SNP array result visualized for a segment of chromosome 17 showing absence of deletions or duplications (top) and a RoH from 17q25.3 to 17qter (bottom). (E) Sanger sequencing of exon 1, demonstrating the presence of the c.-113+2T>A variant. (F) Cartoon of the generated constructs ranging from *GAA* exon 1A to exon 3, with the c.-113+2T>A variant indicated. (G) qRT-PCR of *GAA* exon 2 performed on cDNA obtained from HEK293T cells after transfection with the minigene model. Results are normalized for neomycin. All comparisons were significant: $p < 0.001$. (H) RT-PCRs performed on cDNA obtained from transfected HEK293T. RT-PCR ranging from exon 1b to exon 3 (left) and RT-PCR for the exon1a–1b splice junction (right). With an accompanying cartoon for the RT-PCRs, the location of the primers are indicated using arrows. (I) Cartoon of the disease-associated variant c.-113+2T>A and the pseudodeficiency variant c.2065G>A, both at a homozygous state in patient 3. Error bars in C and G indicate standard deviation (S.D.)

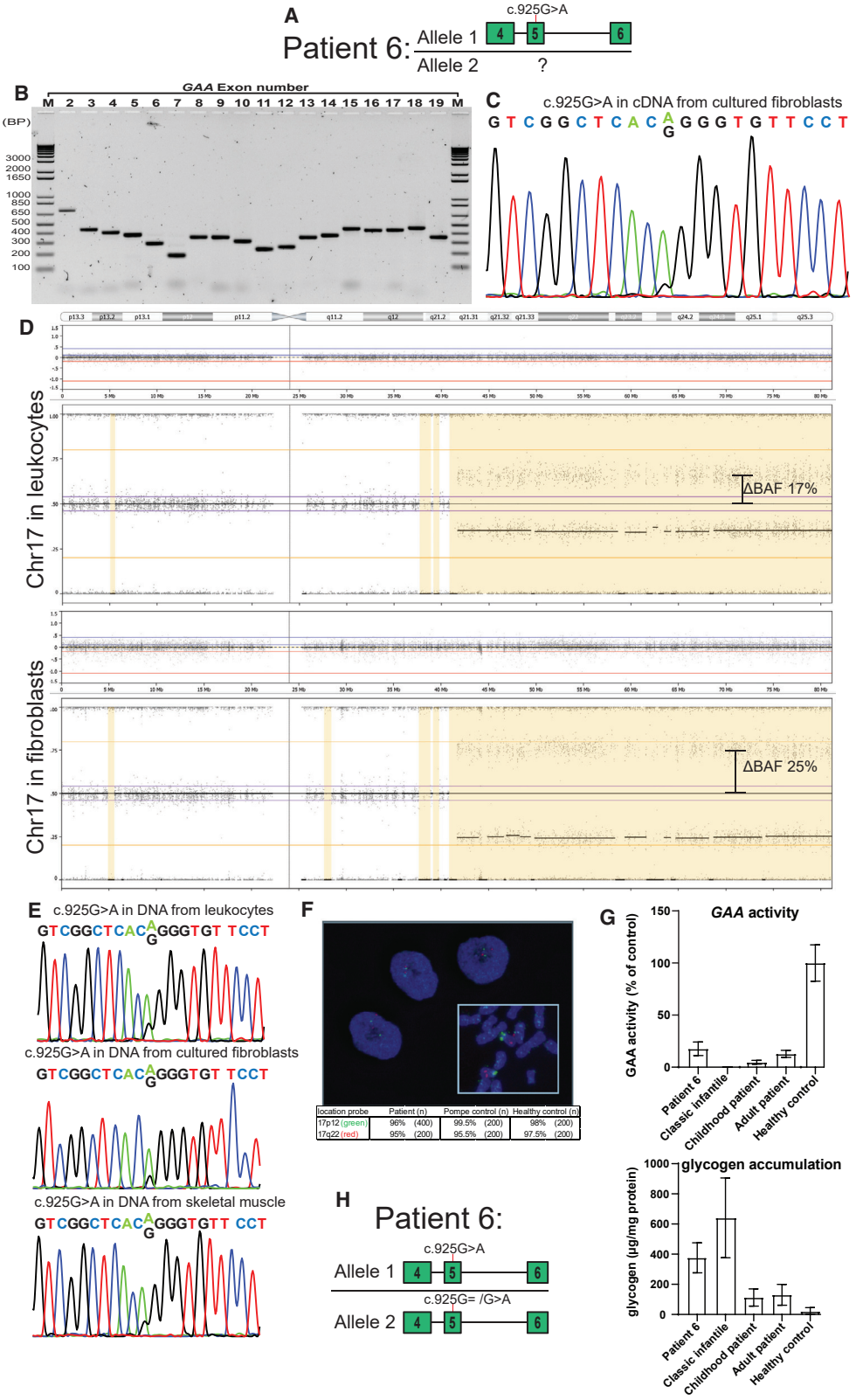

(legend on next page)

Table 2. Clinical and Molecular Information Accompanying Patient 6

Patient Information		
Age at analysis	2.5 months to 4 years	
Gender	male	
	GAA Activity	Patient Range
Fibroblasts	8.1 nmol/h/mg	0–20 nmol/h/mg
Leukocytes	26 nmol/h/mg	0–10 nmol/h/mg
Clinical Description		
Left ventricular hypertrophy detected		
No signs of respiratory insufficiency		
No muscle weakness		
Cardiac Muscle Measurements		
Left ventricular mass	122.1 g (*Z* score +3.7)	
Shortening fraction	37.1% (*Z* score +0.14)	
CK levels	243 U/L (ref < 230 U/L)	
Disease-Associated Variants		
Allele 1	c.925G>A	
Allele 2	no variant found	
Parental Disease-Associated Variants		
Father (Asymptomatic)		
Allele 1	c.925G>A	
Allele 2	no variant found	
Mother (Asymptomatic)		
Allele 1	no variant found	
Allele 2	no variant found	
SNP Array Result		
Segmental abnormality range: Chr17:41.681.527–Chr17qter		

decreased in leukocytes, whereas in primary fibroblasts, enzymatic activity was within the range of late-onset Pompe disease (Table 2).[17] Histochemical analysis of a muscle biopsy showed normal morphology, but some enlarged lysosomes were visible using acid phosphatase staining (Figure S3). In addition, periodic acid-Schiff (PAS) staining showed minor glycogen accumulation (Figure S3). These findings suggested that the patient might have late-onset Pompe disease,[24] but there were two inconsistencies: the lack of GAA deficiency in lymphocytes and the LVH, a characteristic of the classic infantile phenotype but not late-onset Pompe disease. Sanger sequencing revealed only the disease-associated variant c.925G>A at a heterozygous state (Figure 4A). This variant is associated with the classic infantile phenotype when combined with a null allele.[25,26] Sanger sequence analysis of the parents (both showed no signs of Pompe disease) found the c.925G>A only in a heterozygous state in paternal DNA. No other disease-associated variants were identified in the patient nor in his parents (Table 2). Exon-flanking RT-PCR of cDNA from primary fibroblasts of the patient did not detect any splicing aberrations (Figure 4B). Sequence analysis of the *GAA* mRNA transcripts showed that the majority of transcripts contained the c.925G>A variant (Figure 4C). This indicated that the second *GAA* allele was present but was expressed at reduced levels. SNP array analysis identified a 39.5-Mb allelic imbalance, ranging from 17q21.31 to the 17qter (Figure 4D).[17] The imbalance showed no change in CNV but a change in chromosomal equilibrium (i.e., a change in the B allele frequency of heterozygous SNPs) for SNPs located in the affected segment.[17] Within the imbalanced segment, *GAA* was present, whereas all other genes present within this region were unlikely to be the cause of the presented phenotype (Table S1).[27] When analyzing the SNP array data, it became clear that the allelic imbalance was more profound in fibroblasts compared to leukocytes. We estimated a deviation in B allele frequency (ΔBAF) of ±25% in fibroblasts compared to ±17% in leukocytes (Figure 4D). This was consistent with the GAA activity, which showed that activity in fibroblasts was lower compared to leukocytes (Table 2).

Additional Sanger sequence analysis of the patient's tissues showed a skewed contribution in favor of the c.925A variant in primary fibroblasts, leukocytes, and also in skeletal muscle tissue (Figure 4E). Microsatellite analysis of chromosome 17 showed a skewed composition in favor of the paternal allele in the affected segment, whereas markers located in the unaffected segment were distributed evenly (Figure S4). Fluorescence *in situ* hybridization (FISH), using probes located on 17p12 and 17q22 to detect both ends of chromosome 17, showed a normal karyotype in the patient's fibroblasts (Figure 4F). Both ends of the chromosome were present at equal numbers, confirming that this imbalance is not the result of a change in genomic copy number.

The results are in line with a mosaic segmental UPD, in which affected cells contain two copies of the paternal *GAA* that harbor the c.925G>A variant. The patient's tissue is comprised of two distinct cell populations: one with the c.925G>A variant in a homozygous state, resulting in a classic infantile Pompe genotype, and one with

Figure 4. Identification of a Mosaic Segmental UPD in Patient 6

(A) Genotype of patient 6 at the start of analysis. (B) Splicing assay for *GAA* exons 2–19 performed on cDNA obtained from fibroblasts. (C) Sanger sequencing around the c.925G>A variant performed on cDNA obtained from fibroblasts. (D) SNP array analysis of chromosome 17 performed on DNA obtained from leukocytes (top) or fibroblasts (bottom). ΔBAF indicates the estimated difference in BAF between the affected and unaffected segment. (E) Sanger sequencing around the 925G>A variant performed on DNA obtained from leukocytes (top), fibroblasts (middle), or skeletal muscle tissue (bottom). (F) FISH analysis performed in fibroblasts showing probes located on 17p12 (green) and 17q22 (red) and 4′,6-diamidino-2-phenylindole (DAPI) staining to highlight the cell nucleus. A representative image is shown, and a quantification is given below the figure. (G, top) Biochemical quantification of GAA activity measured using 4MU as a substrate. Significance comparing patient 6 and all other samples: not significant. Significance comparing classic infantile and healthy control: $p = 0.01$. (G, bottom) Measurements of intracellular glycogen. Significance comparing classic infantile versus the childhood, adult, and healthy control samples: $p < 0.01$. Comparison of patient 6 and all other samples: not significant (patient 6 versus healthy control: $p = 0.052$). Both assays were performed on the same protein extracts obtained from fibroblasts after culturing to confluence for 3 weeks, followed by a 24h starvation to clear intracellular glycogen. GAA activity is shown as a percentage of the healthy control fibroblasts. (H) Cartoon of both disease-associated variants identified in patient 6. Error bars in G indicate S.D.

Table 3. Novel Variants Identified with Proof of Pathogenicity

	Disease-Associated Variant on Allele 1	Disease-Associated Variant/Event on Allele 2	Proof of Pathogenicity for Novel Variant
Patient 1	c.2331+2T>A	c.1327-61_1437+171del[a]	resulting deletion in the transcript is known to cause a deficiency of *GAA*
Patient 2	c.-32-13T>G	17 kb deletion, including promoter and transcription start site of *GAA*[a]	no RNA expression originating from the allele containing the deletion
Patients 3, 4, and 5	c.-113+2T>A[a] + c.2065G>A[b]	c.-113+2T>A[a] + c.2065G>A[b]	expression and splicing analysis of variant in minigene model
Patient 6	c.925G>A	mosaicism c.925G>A[a]	SNP arrays of different tissues, Sanger sequencing, glycogen accumulation assay

[a]Novel variants.
[b]Pseudodeficiency variant.

the c.925G>A variant in a heterozygous state, which results in a healthy cell population. To confirm this further, two protein-based assays were performed to examine the biochemical properties of the patient's cells. Figure 4G shows the results of the glycogen accumulation and GAA activity assays, which were performed on the same cellular extract. Patient fibroblasts accumulated intracellular glycogen, a characteristic that normally only occurs *in vitro* in fibroblasts derived from classic infantile Pompe patients but not in late-onset patients. However, GAA enzymatic activity (Figure 4G) was present and in the range of late-onset Pompe disease. This is in agreement with a genetic mosaicism with the sample consisting of two cell populations: one that accumulates glycogen *in vitro* and one that still possesses enzymatic GAA activity and thereby does not accumulate glycogen.

In summary, the atypical phenotype for Pompe disease presented by patient 6 can be explained by a genetic mosaicism for a segment of chromosome 17 that includes *GAA*. It is likely that in cardiac cells, the contribution of homozygous cells to heart tissue is relatively large, causing a LVH. In skeletal muscle cells, the mixture of homozygous and heterozygous nuclei in muscle fibers likely causes only mild pathology.

DISCUSSION

Conventional diagnostic procedures are able to identify and diagnose most individuals with Pompe disease; however, a number of cases remain unexplained.[4] Here, we emphasize the need to introduce new methods in the diagnostic validation of Pompe disease in cases for which conventional procedures prove insufficient. With the use of extended diagnostic analyses, we identified three new variants in the *GAA* gene. With the use of minor adjustments to already-existing assays, we proved the pathogenicity of the variants and completed the diagnosis for six cases of Pompe disease derived from four families (Table 3).

In previous work, the exon-flanking RT-PCR analysis proved useful to identify novel variants located outside the coding regions, for example, as shown by the identification of c.2190-345A>G.[9] Here, we showed this assay to be capable of detecting novel deletions and revealing differential gene expression as a result of *GAA* variants. However, the 17kb deletion in patient 2 and thereby other deletions spanning more than one exon remained undetected, and additional assays were required. To detect the deletion of exon 18, which is a common variant in Caucasian patients with Pompe disease, our diagnostic center performs a separate PCR reaction.[28] However, other large deletions are not routinely analyzed and will therefore not be identified. This is supported by the under-representation of gross deletions and other types of variants, such as promoter variants in *GAA*.[10,29,30] As described in the Human Gene Mutation Database (HGMD), gross deletions represent 7.5% of all disease-associated variants, whereas approximately 1% of all disease-associated variants are reported to be located in promoter regions genome wide.[29] For Pompe disease, gross deletions constitute only 1.5% of known variants, and the variants described here in patients 2 and 3 represent the first reported disease-associated variants located in the promoter and 5′ UTR regions of *GAA*.[10] These regions are critical for the regulation of gene expression, and we recommend these regions to be included in future diagnostic analyses. The detection of non-coding variants can be improved with the implementation of techniques already established in many diagnostic laboratories as a follow-up to DNA sequencing. SNP array analysis allows for the detection of large deletions or duplications, whereas aberrant splicing events or severe reductions in gene expression can be detected using whole transcriptome sequencing.[18,31] Other existing techniques can also be implemented for specific monogenic disorders and are capable of detecting smaller aberrations. Multiplex ligation-dependent probe amplification (MLPA) can detect deletions affecting single exons, whereas exon-flanking RT-PCR can be performed to detect deletions, splicing aberrations, and differential gene expression.[9,18] A more systematic approach, as described above, could lead to the identification of new disease-associated variants and provide a complete DNA diagnosis for patients. The implementation of the approaches outlined here should therefore be considered to improve the genetic analysis of cases with an unexplained genetic diagnosis.

Patients with an atypical phenotype often represent a challenge when diagnosing genetic disorders. Patient 6 presented a unique pathological condition: LVH, a characteristic usually observed only in the classic infantile phenotype, while lacking any sign of muscle weakness after 4 years of age. This phenotype was corroborated by the differences in

GAA activity in the patient's tissues. With the use of the SNP array analysis, we detected a chromosomal imbalance on chromosome 17, which was crucial to identify the genetic mosaicism of Pompe disease. Genetic mosaicisms are often associated with a milder symptomatology due to the presence of a healthy or less affected cell population.[32]

The mosaicism in patient 6 appears to be the result of a segmental UPD. UPDs have been associated with many inherited disorders and appropriately explain a subset of patients carrying homozygous disease-associated variants.[33] Whole-chromosome UPDs are reported to occur in 1/3,500 births,[33] whereas segmental UPDs occur less frequently and are the result of somatic recombination.[34–36] The mosaic nature of the segmental UPD and the high percentage of affected cells in several of the patient tissues suggest that the recombination event occurred early in the postzygotic stage of embryonal development.[34–36] Tissues of this patient were thereafter comprised of two cell populations, with the c.925G>A disease-associated variant being present at either a heterozygous (healthy) or homozygous (classic infantile) state.

The presence of a population of healthy cells in the patient did not prevent the development of LVH, which normally only occurs in classic infantile patients. However, at 4 years of age, the patient has not yet manifested any other symptoms related to Pompe disease. The lack of muscle weakness in this patient was reflected by mild pathology in his muscle biopsies. This is likely due to the multinucleation of muscle fibers, whereby the genetic mosaicism in this patient is offset by the presence of both affected and unaffected nuclei in individual muscle fibers, which could be sufficient to prevent muscle pathology. A comprehensive follow-up of this patient, including CNS magnetic resonance imaging (MRI) and neuropsychological investigations, will be required to rule out additional symptoms, such as white matter changes in the brain, which can manifest in classic infantile Pompe patients.[37,38]

This study shows the need for the implementation of additional diagnostic assays and research as a follow-up when conventional procedures prove insufficient or when a patient's symptoms or biochemical characteristics do not match to a disorder. For monogenic disorders, such as Pompe disease, more specific assays can be implemented for an improved analysis of a singular gene. The implementation of this follow-up will likely result in the identification of novel variants and provide a complete DNA diagnosis for patients carrying non-coding variants.

MATERIALS AND METHODS

Patients

The patients described here were selected for their clinical and/or biochemical diagnosis that could be attributed to a deficiency of GAA. Informed consents were obtained to perform extended diagnostic assays to identify *GAA* variants and explain the presented phenotypes. Analysis of the patients analyzed in this study was approved by the medical ethics committee of the Erasmus MC. Primary fibroblasts were not available for patient 4 and 5, assays were performed for patient 3, and findings were thereafter confirmed in DNA from patients 4 and 5.

DNA Analysis

GenBank: NM_001079803.2 and NM_0001079803.2 were used as reference sequences for *GAA* DNA and mRNA, respectively, where c.1 represents the first nucleotide of the translation start codon ATG. NP000143.2 was used as a reference for GAA protein. We note that in previous annotations, exon 1 comprised 334 nt, whereas in current annotations, this region is divided into two exons (exon 1A and 1B) and a 185-nt intron. All SNP arrays analyses were performed using the Illumina Infinium CytoSNP-850K BeadChip platform. Analysis of genes related to genetic disorders located within specified genomic regions was performed using Genomic Oligoarray and SNP Array Evaluation Tool v3.0.

Histology and Imaging

Acid phosphatase staining was performed on cryosections, as described.[39] PAS staining was performed on sections of glycolmethacrylate (GMA)-processed tissue.[24] Hematoxylin and eosin (H&E) stainings were performed on both GMA fixated and cryosections. A Hamamatsu NanoZoomer 2.0 (Hamamatsu Photonics) was used for imaging, and images were analyzed with NDP.view software.

RNA Isolation and cDNA Synthesis

Total RNA was isolated from cultured fibroblasts using the RNeasy minikit (QIAGEN), including a DNaseI (QIAGEN) treatment. RT-PCR was performed using the iScript cDNA synthesis kit (Bio-Rad) in reactions with 300–800 ng RNA input.

PCR and Sanger Sequencing

RT-PCR and qRT-PCR were performed as described.[9] Sanger sequencing of PCR products was performed using a ABI3730XL DNA analyzer (Thermo Fisher Scientific) and analyzed using ApE software.

Generation of the Minigene Constructs and Transfection

The minigene model described in Bergsma et al.[12] was modified as follows: with the use of a primer with a XhoI overhang and a SBF1 restriction site, the exon 1a region was amplified and cloned in the construct. We used the QuikChange II Site-Directed Mutagenesis Kit (Agilent Technologies) to introduce the c.-113+2T>A variant. Transfection of the minigene constructs was performed in HEK293T cells using Lipofectamine 2000 (Invitrogen). RNA was harvested 48 h after transfection.

Enzyme Activity and Glycogen Assay

GAA activity was measured in leukocytes or fibroblasts using 4MU, as described.[9] All 4MU assays were performed in diagnostic settings, with the exception of Figure 4G. For this experiment, fibroblasts had been confluent for 3 weeks and starved in glucose-free medium, 24 h before harvest, after which, GAA activity was measured using the

4MU.[9] Intracellular glycogen was measured with a two-step protocol using amylase and glucose-oxidase.[9]

Fragment Analysis of Microsatellite Markers

15 probes were selected for their location on chromosome 17. Analysis of the VIC- or FAM-labeled products was performed using an ABI3730XL DNA analyzer (Thermo Fisher Scientific).

Fluorescence *In Situ* Hybridization Analysis

FISH was performed on cultured fibroblasts at a low passage number. Two probes located on 17p12 and 17q22 were used to visualize both ends of the chromosome. The cells were not confluent when fixed and classified as having a normal karyotype when two or four copies of each probe were visible.

Statistics

Data were analyzed using IBM SPSS statistics, version 26. For all experiments, normal distribution of data was determined based on calculated residuals. Significance between normally distributed data from two groups was tested using an unpaired two-tailed t test. For experiments with three or more groups, a one-way ANOVA of independent samples with Tukey honestly significant difference (HSD) or Games-Howell post hoc multiple correction (depending on homogeneity of the variance) was performed. Non-normal distributed data were statistically tested using the Kruskal-Wallis method of independent samples with Bonferroni multiple comparison for three or more groups. A p value of less than 0.05 was considered significant for all tests.

SUPPLEMENTAL INFORMATION

Supplemental Information can be found online at https://doi.org/10.1016/j.omtm.2019.12.016.

AUTHOR CONTRIBUTIONS

Conceptualization, S.L.M.i.G., A.T.v.d.P., A.J.B., and W.W.M.P.P.; Methodology, S.L.M.i.G., D.O.S.d.F., and A.J.B.; Validation Verification, M.-A.B.R., and P.W.; Formal Analysis, S.L.M.i.G., A.I., and J.J.S.; Investigation, S.L.M.i.G., D.O.S.d.F., H.D., T.D., and G.M.S.-B.; Resources, T.D., P.W., and M.-A.B.R.; Data Curation, H.D., J.J.S., and A.d.K.; Writing – Original Draft, S.L.M.i.G. and A.I.; Writing – Review & Editing, all authors; Supervision Project Administration, A.J.B., J.M.P.v.d.H., L.H.H., and W.W.M.P.P.; Funding Acquisition, A.T.v.d.P. and W.W.M.P.P.

CONFLICTS OF INTEREST

A.T.v.d.P. has provided consulting services for various industries in the field of Pompe disease under an agreement between these industries and Erasmus MC, Rotterdam, the Netherlands. All other authors declare no competing interests.

ACKNOWLEDGMENTS

We thank the members of the Molecular Stem Cell Biology Group for the critical discussions. This work was funded through Conselho Nacional de Desenvolvimento Científico e Tecnológico (CNPq; Brazil), the Sophia Foundation for Medical Research (SSWO; project number s17-32), and Metakids (project number 2016 - 063). This project has received funding from the Ministry of Economic Affairs under TKI allowance under the TKI-Programme Life Sciences & Health. The collaboration project is co-funded by the PPP Allowance made available by Health ~ Holland, Top Sector Life Sciences & Health, to stimulate public-private partnerships (project numbers LSHM16008 and LSHM19015). The collaboration project is co-initiated by the Prinses Beatrix Spierfonds.

REFERENCES

1. Güngör, D., and Reuser, A.J. (2013). How to describe the clinical spectrum in Pompe disease? Am. J. Med. Genet. A. *161A*, 399–400.
2. Prater, S.N., Patel, T.T., Buckley, A.F., Mandel, H., Vlodavski, E., Banugaria, S.G., Feeney, E.J., Raben, N., and Kishnani, P.S. (2013). Skeletal muscle pathology of infantile Pompe disease during long-term enzyme replacement therapy. Orphanet J. Rare Dis. *8*, 90.
3. Van den Hout, H., Reuser, A.J., Vulto, A.G., Loonen, M.C., Cromme-Dijkhuis, A., and Van der Ploeg, A.T. (2000). Recombinant human alpha-glucosidase from rabbit milk in Pompe patients. Lancet *356*, 397–398.
4. van der Ploeg, A.T., Kruijshaar, M.E., Toscano, A., Laforêt, P., Angelini, C., Lachmann, R.H., Pascual Pascual, S.I., Roberts, M., Rösler, K., Stulnig, T., et al.; European Pompe Consortium (2017). European consensus for starting and stopping enzyme replacement therapy in adult patients with Pompe disease: a 10-year experience. Eur. J. Neurol. *24*, 768–e31.
5. Goldstein, J.L., Young, S.P., Changela, M., Dickerson, G.H., Zhang, H., Dai, J., Peterson, D., Millington, D.S., Kishnani, P.S., and Bali, D.S. (2009). Screening for Pompe disease using a rapid dried blood spot method: experience of a clinical diagnostic laboratory. Muscle Nerve *40*, 32–36.
6. Burton, B.K., Kronn, D.F., Hwu, W.L., and Kishnani, P.S.; Pompe Disease Newborn Screening Working Group (2017). The Initial Evaluation of Patients After Positive Newborn Screening: Recommended Algorithms Leading to a Confirmed Diagnosis of Pompe Disease. Pediatrics *140* (*Suppl 1*), S14–S23.
7. Labrousse, P., Chien, Y.H., Pomponio, R.J., Keutzer, J., Lee, N.C., Akmaev, V.R., Scholl, T., and Hwu, W.L. (2010). Genetic heterozygosity and pseudodeficiency in the Pompe disease newborn screening pilot program. Mol. Genet. Metab. *99*, 379–383.
8. Kishnani, P.S., Steiner, R.D., Bali, D., Berger, K., Byrne, B.J., Case, L.E., Crowley, J.F., Downs, S., Howell, R.R., Kravitz, R.M., et al. (2006). Pompe disease diagnosis and management guideline. Genet. Med. *8*, 267–288.
9. Bergsma, A.J., Kroos, M., Hoogeveen-Westerveld, M., Halley, D., van der Ploeg, A.T., and Pijnappel, W.W. (2015). Identification and characterization of aberrant GAA pre-mRNA splicing in pompe disease using a generic approach. Hum. Mutat. *36*, 57–68.
10. Niño, M.Y., In 't Groen, S.L.M., Bergsma, A.J., van der Beek, N.A.M.E., Kroos, M., Hoogeveen-Westerveld, M., van der Ploeg, A.T., and Pijnappel, W.W.M.P. (2019). Extension of the Pompe mutation database by linking disease-associated variants to clinical severity. Hum. Mutat. *40*, 1954–1967.
11. Bergsma, A.J., In 't Groen, S.L.M., van den Dorpel, J.J.A., van den Hout, H.J.M.P., van der Beek, N.A.M.E., Schoser, B., Toscano, A., Musumeci, O., Bembi, B., Dardis, A., et al. (2019). A genetic modifier of symptom onset in Pompe disease. EBioMedicine *43*, 553–561.
12. Bergsma, A.J., In 't Groen, S.L., Verheijen, F.W., van der Ploeg, A.T., and Pijnappel, W.W.M.P. (2016). From Cryptic Toward Canonical Pre-mRNA Splicing in Pompe Disease: a Pipeline for the Development of Antisense Oligonucleotides. Mol. Ther. Nucleic Acids *5*, e361.
13. van der Wal, E., Bergsma, A.J., van Gestel, T.J.M., In 't Groen, S.L.M., Zaehres, H., Araúzo-Bravo, M.J., Schöler, H.R., van der Ploeg, A.T., and Pijnappel, W.W.M.P. (2017). GAA Deficiency in Pompe Disease Is Alleviated by Exon Inclusion in iPSC-Derived Skeletal Muscle Cells. Mol. Ther. Nucleic Acids *7*, 101–115.

14. van der Wal, E., Bergsma, A.J., Pijnenburg, J.M., van der Ploeg, A.T., and Pijnappel, W.W.M.P. (2017). Antisense Oligonucleotides Promote Exon Inclusion and Correct the Common c.-32-13T>G GAA Splicing Variant in Pompe Disease. Mol. Ther. Nucleic Acids *7*, 90–100.

15. Bergsma, A.J., van der Wal, E., Broeders, M., van der Ploeg, A.T., and Pim Pijnappel, W.W.M. (2018). Alternative Splicing in Genetic Diseases: Improved Diagnosis and Novel Treatment Options. Int. Rev. Cell Mol. Biol. *335*, 85–141.

16. Eggermann, T., Soellner, L., Buiting, K., and Kotzot, D. (2015). Mosaicism and uniparental disomy in prenatal diagnosis. Trends Mol. Med. *21*, 77–87.

17. Labrijn-Marks, I., Somers-Bolman, G.M., In 't Groen, S.L.M., Hoogeveen-Westerveld, M., Kroos, M.A., Ala-Mello, S., Amaral, O., Miranda, C.S., Mavridou, I., Michelakakis, H., et al. (2019). Segmental and total uniparental isodisomy (UPiD) as a disease mechanism in autosomal recessive lysosomal disorders: evidence from SNP arrays. Eur. J. Hum. Genet. *27*, 919–927.

18. Silva, M., de Leeuw, N., Mann, K., Schuring-Blom, H., Morgan, S., Giardino, D., Rack, K., and Hastings, R. (2019). European guidelines for constitutional cytogenomic analysis. Eur. J. Hum. Genet. *27*, 1–16.

19. Bali, D.S., Goldstein, J.L., Banugaria, S., Dai, J., Mackey, J., Rehder, C., and Kishnani, P.S. (2012). Predicting cross-reactive immunological material (CRIM) status in Pompe disease using GAA mutations: lessons learned from 10 years of clinical laboratory testing experience. Am. J. Med. Genet. C. Semin. Med. Genet. *160C*, 40–49.

20. Boerkoel, C.F., Exelbert, R., Nicastri, C., Nichols, R.C., Miller, F.W., Plotz, P.H., and Raben, N. (1995). Leaky splicing mutation in the acid maltase gene is associated with delayed onset of glycogenosis type II. Am. J. Hum. Genet. *56*, 887–897.

21. Dardis, A., Zanin, I., Zampieri, S., Stuani, C., Pianta, A., Romanello, M., Baralle, F.E., Bembi, B., and Buratti, E. (2014). Functional characterization of the common c.-32-13T>G mutation of GAA gene: identification of potential therapeutic agents. Nucleic Acids Res. *42*, 1291–1302.

22. Genome of the Netherlands Consortium (2014). Whole-genome sequence variation, population structure and demographic history of the Dutch population. Nat. Genet. *46*, 818–825.

23. Kroos, M.A., Mullaart, R.A., Van Vliet, L., Pomponio, R.J., Amartino, H., Kolodny, E.H., Pastores, G.M., Wevers, R.A., Van der Ploeg, A.T., Halley, D.J., and Reuser, A.J. (2008). p.[G576S; E689K]: pathogenic combination or polymorphism in Pompe disease? Eur. J. Hum. Genet. *16*, 875–879.

24. Schaaf, G.J., van Gestel, T.J., Brusse, E., Verdijk, R.M., de Coo, I.F., van Doorn, P.A., van der Ploeg, A.T., and Pijnappel, W.W. (2015). Lack of robust satellite cell activation and muscle regeneration during the progression of Pompe disease. Acta Neuropathol. Commun. *3*, 65.

25. Kroos, M.A., van Leenen, D., Verbiest, J., Reuser, A.J., and Hermans, M.M. (1998). Glycogen storage disease type II: identification of a dinucleotide deletion and a common missense mutation in the lysosomal alpha-glucosidase gene. Clin. Genet. *53*, 379–382.

26. Markic, J., Polic, B., Stricevic, L., Metlicic, V., Kuzmanic-Samija, R., Kovacevic, T., Ivkosic, I.E., and Mestrovic, J. (2014). Effects of immune modulation therapy in the first Croatian infant diagnosed with Pompe disease: a 3-year follow-up study. Wien. Klin. Wochenschr. *126*, 133–137.

27. Wierenga, K.J., Jiang, Z., Yang, A.C., Mulvihill, J.J., and Tsinoremas, N.F. (2013). A clinical evaluation tool for SNP arrays, especially for autosomal recessive conditions in offspring of consanguineous parents. Genet. Med. *15*, 354–360.

28. Van der Kraan, M., Kroos, M.A., Joosse, M., Bijvoet, A.G., Verbeet, M.P., Kleijer, W.J., and Reuser, A.J. (1994). Deletion of exon 18 is a frequent mutation in glycogen storage disease type II. Biochem. Biophys. Res. Commun. *203*, 1535–1541.

29. Stenson, P.D., Mort, M., Ball, E.V., Evans, K., Hayden, M., Heywood, S., Hussain, M., Phillips, A.D., and Cooper, D.N. (2017). The Human Gene Mutation Database: towards a comprehensive repository of inherited mutation data for medical research, genetic diagnosis and next-generation sequencing studies. Hum. Genet. *136*, 665–677.

30. Cooper, D.N. (2002). Human gene mutation in pathology and evolution. J. Inherit. Metab. Dis. *25*, 157–182.

31. Gonorazky, H.D., Naumenko, S., Ramani, A.K., Nelakuditi, V., Mashouri, P., Wang, P., Kao, D., Ohri, K., Viththiyapaskaran, S., Tarnopolsky, M.A., et al. (2019). Expanding the Boundaries of RNA Sequencing as a Diagnostic Tool for Rare Mendelian Disease. Am. J. Hum. Genet. *104*, 1007.

32. Dipple, K.M., and McCabe, E.R. (2000). Phenotypes of patients with "simple" Mendelian disorders are complex traits: thresholds, modifiers, and systems dynamics. Am. J. Hum. Genet. *66*, 1729–1735.

33. Yamazawa, K., Ogata, T., and Ferguson-Smith, A.C. (2010). Uniparental disomy and human disease: an overview. Am. J. Med. Genet. C. Semin. Med. Genet. *154C*, 329–334.

34. Kotzot, D. (2008). Complex and segmental uniparental disomy updated. J. Med. Genet. *45*, 545–556.

35. Robinson, W.P. (2000). Mechanisms leading to uniparental disomy and their clinical consequences. BioEssays *22*, 452–459.

36. Kearney, H.M., Kearney, J.B., and Conlin, L.K. (2011). Diagnostic implications of excessive homozygosity detected by SNP-based microarrays: consanguinity, uniparental disomy, and recessive single-gene mutations. Clin. Lab. Med. *31*, 595–613, ix.

37. Ebbink, B.J., Aarsen, F.K., van Gelder, C.M., van den Hout, J.M., Weisglas-Kuperus, N., Jaeken, J., Lequin, M.H., Arts, W.F., and van der Ploeg, A.T. (2012). Cognitive outcome of patients with classic infantile Pompe disease receiving enzyme therapy. Neurology *78*, 1512–1518.

38. Ebbink, B.J., Poelman, E., Aarsen, F.K., Plug, I., Régal, L., Muentjes, C., van der Beek, N.A.M.E., Lequin, M.H., van der Ploeg, A.T., and van den Hout, J.M.P. (2018). Classic infantile Pompe patients approaching adulthood: a cohort study on consequences for the brain. Dev. Med. Child Neurol. *60*, 579–586.

39. van den Berg, L.E., de Vries, J.M., Verdijk, R.M., van der Ploeg, A.T., Reuser, A.J., and van Doorn, P.A. (2011). A case of adult Pompe disease presenting with severe fatigue and selective involvement of type 1 muscle fibers. Neuromuscul. Disord. *21*, 232–234.